J Appl Electrochem (2014) 44:857–866
DOI 10.1007/s10800-014-0694-y

RESEARCH ARTICLE

Anodic oxidation of butan-1-ol on Pd and Pt electrodes in alkaline medium

Parthasarathi Mukherjee · Swapan Kumar Bhattacharya

Received: 22 November 2013 / Accepted: 28 April 2014 / Published online: 15 May 2014

Abstract Pure Pd is investigated as electro-catalyst for oxidation of butan-1-ol in aqueous NaOH solution and compared with the conventional catalyst, pure Pt. The steady-state anodic current density increases on increasing the potential up to −52 and −3 mV for Pt and Pd, respectively, and it reveals that Pd is a better electro-catalyst than Pt above −0.18 V versus MMO [Hg/HgO/OH^-(0.1 M) having reversible electrode potential of 0.1 V vs. NHE]. Multiple scan cyclic voltammetry also reveals faster poisoning of Pt than Pd electrode. The Tafel slope for Pd (0.511 V dec^{-1}) is lower than Pt (2.30 V dec^{-1}) where as poisoning potential and current density of the former are greater than Pt indicating a relatively higher catalytic activity of Pd electrode. The FTIR study reveals the presence of aldehyde group in the products obtained with Pt unlike Pd electrode indicating different mechanistic pathways followed by them. With increase of potential in the range −200 to 300 mV, the order with respect to butan-1-ol gradually decreases for Pt due to poisoning in the process of formation of complete oxidation product, CO_3^{2-}, but increases for Pd due to faster removal of adsorbed intermediates with the formation of mainly butyrate. In this study, different mechanisms are proposed for Pt and Pd which conform to the experimental results.

Keywords Butan-1-ol electro-oxidation · Catalytic activity of Pt and Pd · Order · FTIR study of products · Mechanism of oxidation

P. Mukherjee · S. K. Bhattacharya (✉)
Physical Chemistry Section, Department of Chemistry, Jadavpur University, Kolkata 700032, India
e-mail: skbhatt7@yahoo.co.in

1 Introduction

The direct alcohol fuel cells (DAFC) with small alcohols as fuel have gathered enormous attraction as potential power sources of portable electronic devices and cars. This is plausibly because of their easy storage, transport, handling, and much higher volumetric energy density than presently used fuels like hydrogen and natural gas [1, 2]. However, the development of methanol fuel cell is facing serious difficulties [3, 4] for its slow electrode kinetics of oxidation, high crossover, volatility, toxicity, etc. Therefore, increasing research efforts with other small alcohols are being carried out to design and develop more efficient catalysts for DAFCs. Notably, significant number of works has been also done on ethanol [3–7] and a few on propanols [8, 9], but very few on butanols [10]. On the other hand, butan-1-ol is less corrosive and has lower crossover current than methanol and ethanol [5–7]. It is less volatile and toxic than methanol and possesses higher flash point of 35 °C which is beneficial for fire safety. In this study, butan-1-ol is investigated as the fuel for DAFCs because it is the most active isomer among all C_4–alcohols [10] and expected to show good performance like $C_{\bar{3}}$ alcohols. The reaction of partial anodic oxidation of butan-1-ol is given by.

$$CH_3CH_2CH_2CH_2OH + 5OH^- = CH_3CH_2CH_2COO^- + 4H_2O + 4e^- \quad (1)$$

So, it can be told from Nernst equation that the reversible potential would be cathodically shifted at high pH. Similar is the case for the reaction of complete oxidation of butan-1-ol. So, the purely thermodynamic consideration predicts that the media of high pH make the reaction favorable. Other advantages in using alkali as the medium are less poisoning, less permeation of alcohol through the

nafion membrane, less depolarization of oxygen cathode, wider possibility of nonmetals as catalysts and co-catalysts, etc. However, due to carbonation, CO_2 is accumulated in the cell in alkaline medium resulting decrease in pH and efficiency of the cell. So, the kinetics in DAFC would be significantly improved [11, 12] if the alcohol electro-oxidation is carried out in the alkaline medium avoiding carbonation.

Pt has been extensively investigated as the electro-catalysts for oxidation of different small alcohols in alkaline medium [13–17], and it is also reported that Pt has a low activity in acid medium [8]. But, the high cost and limited abundance [18] of Pt constitute another major barrier to the development of DAFCs. Pt-free electro-catalysts such as Pd are used for alcohol oxidation in alkaline medium [8, 9, 19]. Pd-based electro-catalysts are used for electro-oxidation of formic acid and hydrazine in acid medium and propan-1-ol, propan-2-ol and formaldehyde in alkaline medium [16, 17]. Such studies and other reports show that Pd-based electrodes are highly active for oxidation of small organic molecules in alkaline medium. So, it favors the potential use of non-noble metals as co-catalyst by choosing alkali as the medium.

On the other hand, despite numerous studies of eletrooxidation of methanol and ethanol on modified Pt and Pd electrodes [19–24], the study of butan-1-ol on pure Pt and Pd is very rare [25]. In this study, pure Pd is investigated as electro-catalyst for butan-1-ol oxidation and compared with the conventional catalyst, pure Pt in alkaline medium. The study of oxidation of butan-1-ol on pure metal catalysts may provide valuable fundamental data for the development of new, highly active modified catalysts for its oxidation in alkaline fuel cells.

2 Experimental

2.1 Reagents and instruments

Analytical grade reagent like NaOH, butan-1-ol and acetone were purchased from Mark, India. Millipore water was used throughout the experiment. All electrochemical measurements were carried out at 25 °C in a three electrode cell using computer-aided Potentiostat/Galvanostat Instrument (AUTOLAB Company). Freshly prepared nitrogen (99.99 %)—purged solution was used in each experiment.

2.2 Electrochemical measurement

The working electrodes were platinum (99.99 %), palladium (99.97 %) wires (Arora Matthey) with a geometrical area of 0.078 and 0.112 cm^2, respectively. A platinum foil having an area of 3.00 cm^2 and $Hg/HgO/OH^-$ (0.1 M) electrode (MMO) was used as counter and reference electrodes for CV study, respectively. The CV study is executed in the potential region of −0.9 to 0.6 V at the scan rates 2–200 mV s^{-1}.The electrolysis of 0.1 M butan-1-ol in 0.1 M NaOH solution was carried out at a current density of 30 μA cm^{-2} in N_2 atmospheres for 72 h using either Pd or Pt electrode as anode and a large Pt electrode as cathode. The resulting solutions were dried in vacuum and the solid samples obtained were used for FTIR study (Perkin Elmer, Spectrum RX1, Resolution 4 cm^{-1}).

3 Result and discussion

3.1 Background cyclic voltammetric study

Figure 1 shows the cyclic voltammogram (CV)s (1st cycle) of the Pt and Pd electrode in 0.1 M NaOH solution with a scan rate(v) of 0.05 V s^{-1} in the potential range from −0.9 to 0.6 V. At the start potential of −0.9 V, hydrogen evolution reaction occurs vigorously for both the electrodes. During anodic sweep, three distinct regions have appeared in CV for both Pt and Pd electrodes, which correspond to three electrochemical processes occurring on the surface of the electrodes. The Fig. 1 reveals that the onset of hydrogen evolution on both Pt and Pd electrodes occurs in the potential region between −0.9 and −0.7 V and the pair of current peaks, P1 for Pt and a broad single peak P1′ for Pd indicates electrochemical desorption of hydrogen according to Eq. (2) of Scheme (1) [20–24]. During reverse scan, a pair of small hydrogen adsorption peaks appears below ca −0.55 V for Pt as shown in the top inset of Fig. 1. Similar peak is absent for Pd plausibly as in situ generated hydrogen goes subsurface of Pd. In the next region during forward scan, the adsorption of OH^- ion commences on both the electrodes following Eq. (3).The corresponding current peaks are P2 and P2′ due to M–OH formation for Pt and Pd, respectively. Peak potential of Pt–OH formation (0.055 V) is more positive than Pd–OH formation (0.005 V) but commencement of OH^- adsorption occurs at more negative potential for Pt(−0.420 V) than Pd(−0.219 V) surface. In the next stage of oxidation, formation of M–O takes place corresponding to P3 and P3′ following Eq. (4) [19, 21, 25–28] of Scheme (1). The onset and peak potentials (Ep) of formation of platinum (II) oxide appear at ca 0.20 and 0.314 V, respectively, and those of Pd appear at ca 0.167 and 0.315 V, respectively. The oxygen evolution reaction occurs at much higher potential following equation (5). On cathodic sweep, one cathodic peak is noticed for each of Pt (P4) and Pd (P4′) other than peaks for hydrogen adsorption for Pt. Peak P4 centered at ca −0.242 V can be attributed to the reduction of Pt(II) oxide

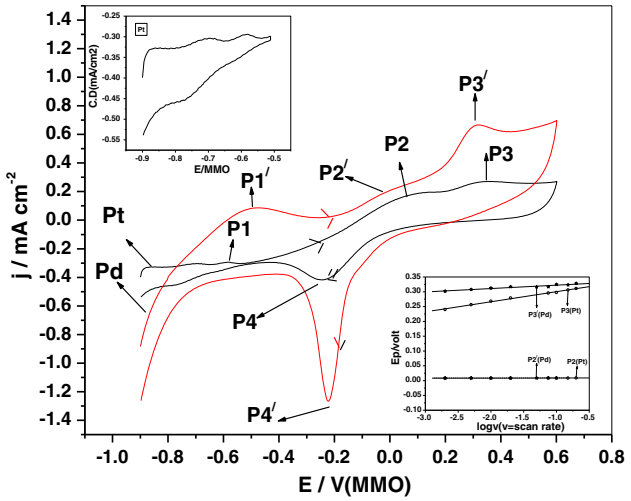

Fig. 1 Cyclic voltammograms (1st cycle) of Pt and Pd electrode in 0.1 M NaOH solution at scan rate, 50 mV s^{-1}. *Top insets* represents plot of C.D (mA cm^{-2}) vs. *E* (MMO) and *bottom inset* represents plot of *E*p/volt vs. log *v* (*v* = scan rate)

$$MH(abs/ads) + OH^- \rightarrow M + H_2O + e^- \text{.....(2)}$$

$$M + OH^- \rightleftharpoons M - OH_{ads} + e^- \text{.....(3)}$$

$$M - OH_{ads} + OH^- \rightarrow M - O + H_2O + e^- \text{.....(4)}$$

$$M - O + 2OH^- \rightarrow M + H_2O + O_2 + 2e^- \text{.....(5)}$$

$$M - O + H_2O + 2e^- \rightleftharpoons M + 2OH^- \text{.....(6)}$$

Scheme 1 Electrochemical reactions occurring on Pt and Pd electrodes in pure alkaline medium

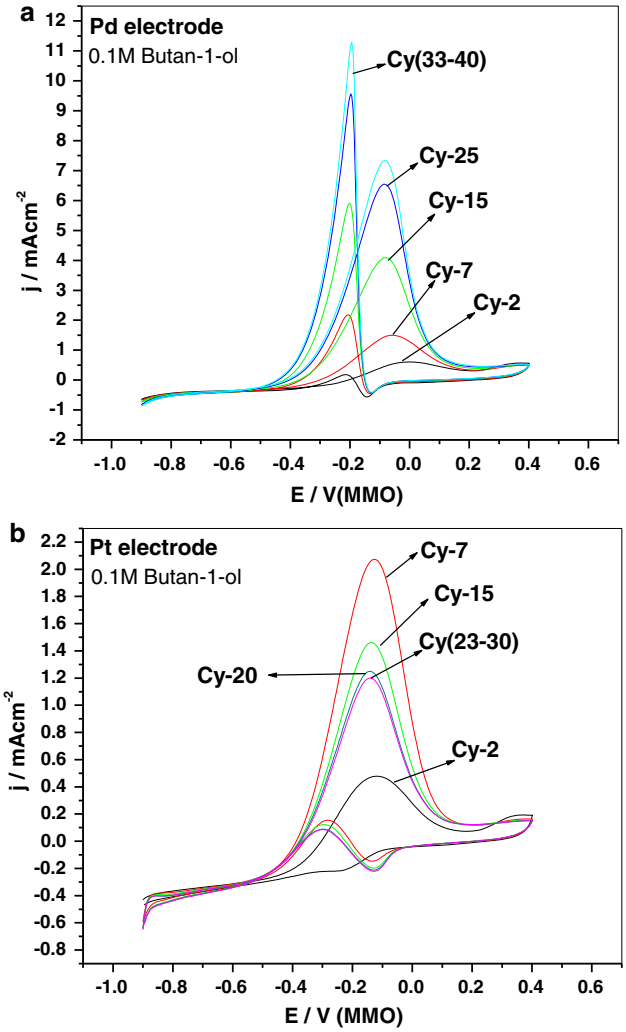

Fig. 2 Cyclic voltammograms of different cycles of **a** Pd and **b** Pt electrodes in 0.1 M butan-1-ol in 0.1 M NaOH at scan rate, 50 mV s^{-1}

to Pt and P4/centered at ca −0.224 V for Pd(II) oxide to Pd following Eq. (6) [8, 29]. The less negative potential for the reduction of Pd–O to Pd than Pt indicates that M–OH is comparatively stable for Pt than Pd seemingly due to greater Pt–O bond strength (246 kJ mol^{-1}) than the Pd–O (56 kJ mol^{-1}) [30, 31], so removal of poisoning in alcohol oxidation reaction utilizing M–OH occurs more easily with Pd than Pt. Since the ratio of peak current densities for $M(OH)_2$ formation $\left(I_{P2'}/I_{P2}\right)$ is about 1.3 (0.217/0.164), it reveals that hydroxylation is kinetically more favorable on Pd. A reversible and irreversible condition is found during the surface oxidation on both Pt and Pd electrodes in sodium hydroxide solution, as presented at the bottom inset of Fig. 1. Constancy of the peak potential of P2/P2/ and P4/P4/ with the change of scan rate, indicates that a reversible reaction occurs in the potential region of P2/P2/ and P4/P4/ of the two electrodes. But the absence of any cathodic peak corresponding to P3/P3/ and the linear variation of the peak potential of P3/P3/ with logarithm of scan rate as shown at the bottom inset of Fig. 1. It suggests the slow irreversible nature of formation of higher valence oxide on both the electrodes. Exactly similar observation is found by Lovic and co-authors [25] with different single crystal surfaces of Pt. In our study with polycrystalline Pt and Pd surfaces the tip of the peaks are somewhat blunt due to merging of different peaks of various crystal planes constituting the polycrystalline surface.

The CVs (Fig. 1) are used for the estimation of Electrochemical Surface Area (ESA) for the Pt and Pd catalyst in alkaline medium. The ESA of Pt catalyst was determined by measuring the charge collected in the hydrogen adsorption/desorption region, after double layer correction. It is a reliable method for computation of ESA for Pt electrode. The charge required for oxidation of single layer

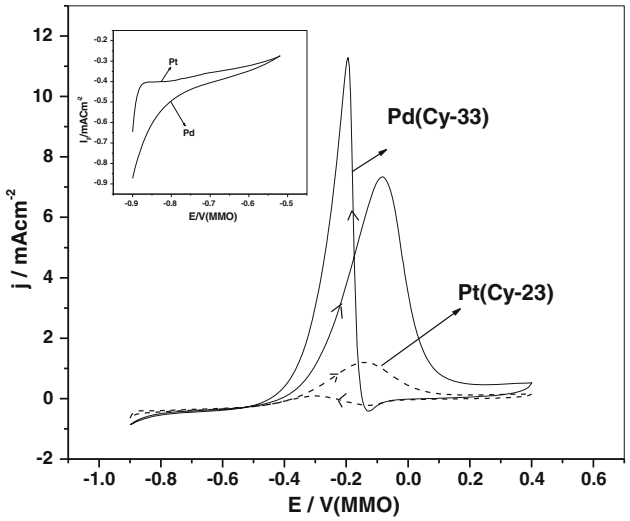

Fig. 3 Cyclic voltammograms of steady cycles of Pt and Pd electrodes in 0.1 M butan-1-ol in 0.1 M NaOH at scan rate, 50 mV s^{-1}. *Inset* represents plot of I_F/mA cm^{-2} vs. *E*/V (MMO)

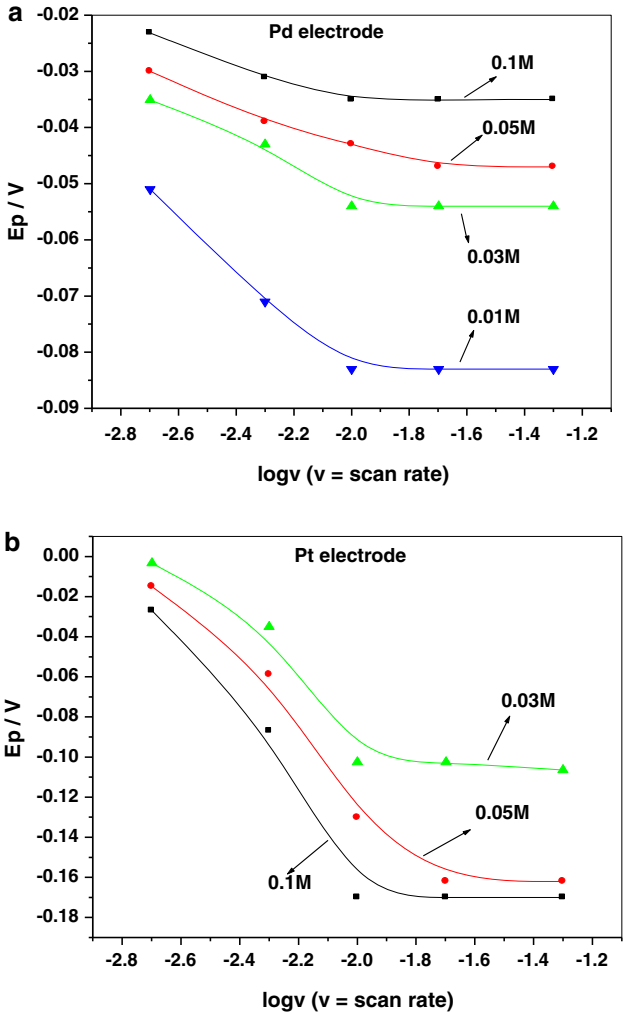

Fig. 4 Plot of peak potential/V vs. log of scan rate for **a** Pd and **b** Pt electrodes immersed in aqueous alkaline solution of butan-1-ol of different concentrations

of hydrogen on Pt surface is assumed to be 210 μC cm^{-2} [32]. The computed ESA value is found to be 0.1952 cm^{-2} and roughness factor is 2.50 for Pt. Hydrogen adsorption method is not applicable for Pd as it significantly dissolves hydrogen which goes into subsurface. The ESA of Pd was measured by determining the coulombic charge for the reduction of Palladium oxide. The charge required for the reduction of Pd–O monolayer is assumed as 405 μC cm^{-2} [33, 34] and the value obtained is 0.2093 cm^{-2} and the roughness factor is 1.87.

3.2 Cyclic voltammetric study of butan-1-ol

In cyclic voltammetric study of butan-1-ol in 0.1 M NaOH solution, multiple triangular sweep of potential is applied. It reveals that the current density at each potential including peak potential gradually increases to reach a steady CV profile at 33 cycles for Pd electrode as displayed in Fig. 2(a). But for Pt, current density initially increases, then decreases and finally a steady CV is attained at cycle 23, as depicted in Fig. 2(b). These figures suggest greater poison tolerance ability of Pd electrode and faster poisoning of Pt during butan-1-ol oxidation reaction.

The steady cyclic voltammogram (Fig. 3) of butan-1-ol oxidation on Pd and Pt electrodes can be easily characterized by two well-defined anodic current peaks on the forward and backward scans of potential. The peak generated during forward scan corresponds to the composite response of the stepwise oxidation of the freshly adsorbed alcohol, while the sharp anodic peak generated in the reverse (backward) scan is associated with the oxidation of freshly adsorbed alcohol and previously adsorbed species [35, 36] after onset of the process of removal of blocking of M–O from the electrode surface. Thus, the magnitude of the current density at different potentials in the forward scan reflects the direct electro-catalytic activity of the electrodes at the potentials for the said oxidation in alkaline medium. It is evident from Fig. 3 that each value of the current density in the forward scan is higher on Pd electrode above ca −0.52 V. It is found that the forward peak current density of Pd (7.31 mA cm^{-2}) is higher than Pt (1.22 mA cm^{-2}). The peak current density ratio is 6 times with respect to geometrical surface area and 3.93/0.488 = 8 times with respect to ESA. The higher forward peak current density of Pd than Pt electrode and

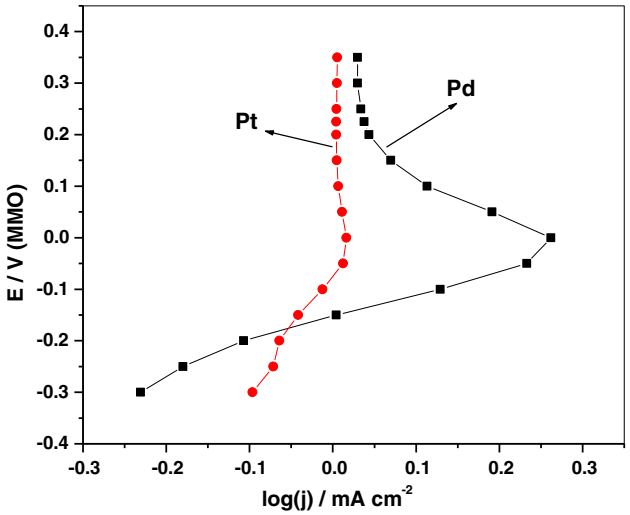

Fig. 5 Tafel plots (potential/V vs. log of current density) for Pt and Pd electrodes immersed in aqueous alkaline solution of butan-1-ol of different concentrations

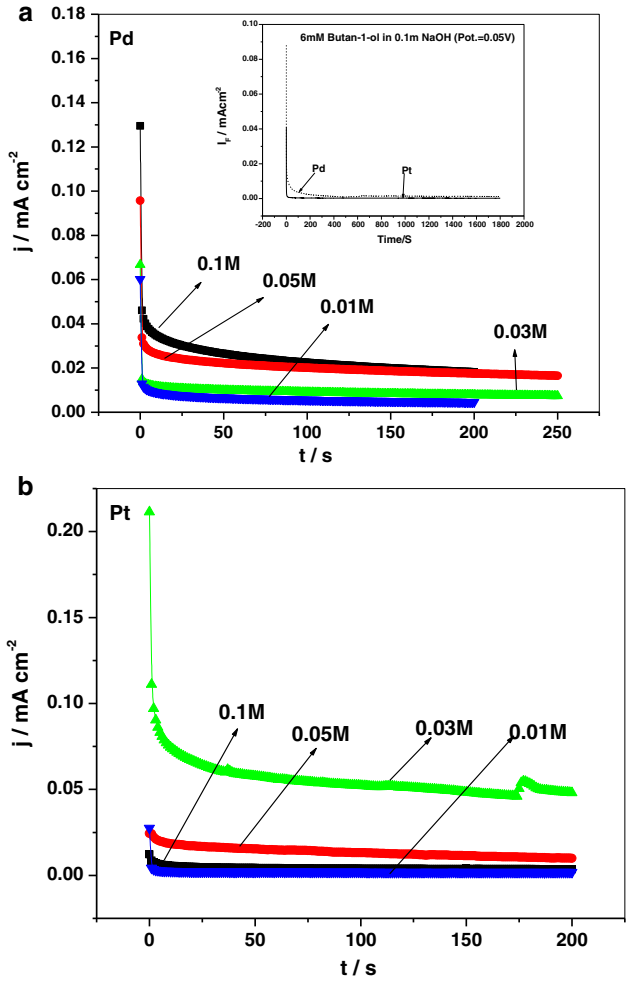

Fig. 6 Chronoamperometric study of **a** Pd and **b** Pt electrodes immersed in aqueous alkaline solution of butan-1-ol of different concentrations. *Inset* of **a** represents plot of I_F/(mA cm^{-2}) vs. time/s

the steeper rise of current density with increasing potential for Pd indicate that Pd exhibits a better catalytic activity than Pt above a certain potential, for anodic oxidation of butan-1-ol in alkaline medium, although ESA of Pd is lower than that of Pt.

Figure 4(a) and (b) illustrate the variation of forward peak potential (E_p) with log of scan rate (v) of potential at different concentrations of butan-1-ol for Pd and Pt electrodes, respectively, reflecting that E_p decreases with increase of scan rate until a constancy is reached in each case, indicating consumption of electrochemical oxidation product on the electrode surface by some relatively slow chemical reactions. Thus, the overall oxidation process seems to undergo a complex and coupled reaction mechanism of E_rC_i type [37] which consists of reversible electrochemical reaction followed by an irreversible chemical reaction for both the systems. In case of Pd, more negative peak potential is found with the lowest concentration (0.01 M) studied and E_p is in the order of butan-1-ol concentration 0.01 M < 0.03 M < 0.05 M < 0.1 M at all scan rates. It indicates that oxidation of carbon-containing intermediates which are oxidized at relatively higher potential are produced more and more on increasing concentration of butan-1-ol. Pd electro-catalyst is suitable for both lower and higher concentration of butan-1-ol at least in the concentration range studied. On the contrary, Ep varies in the order of concentration 0.1 M < 0.05 M < 0.03 M for Pt reflecting that higher concentration is not favorable for oxidation of carbon-containing intermediates on Pt at the potential range studied. This also signifies that butan-1-ol adsorption is relatively higher on Pd surface compared to that on Pt surface. This difference may cause the change in the mechanistic pathway in butan-1-ol electro-oxidation on Pd and Pt electrodes.

The steady-state kinetic parameters for butan-1-ol oxidation in alkaline medium on the two electrodes were determined in the potential range −0.3 to 0.3 V by the Tafel plots, Fig. 5. It is observed that current density increases with potential up to −0.05 V for Pt and 0.0 V for Pd. The surfaces of metals are in the state of saturation with metal hydroxide at the state as evident from Fig. 1. On increasing the potential further current decreases and becomes constant at the potential 0.1 V for Pt and 0.20 V for Pd corresponding to onset of formation of M–O. It indicates that large surface concentration of metal hydroxide is responsible for decreasing of steady-state current for oxidation of butan-1-ol and both metal hydroxide and oxide are the blocking agents as evident from Fig. 5. Moreover, this profile also shows that Pd provides greater current density than Pt above −0.18 V.

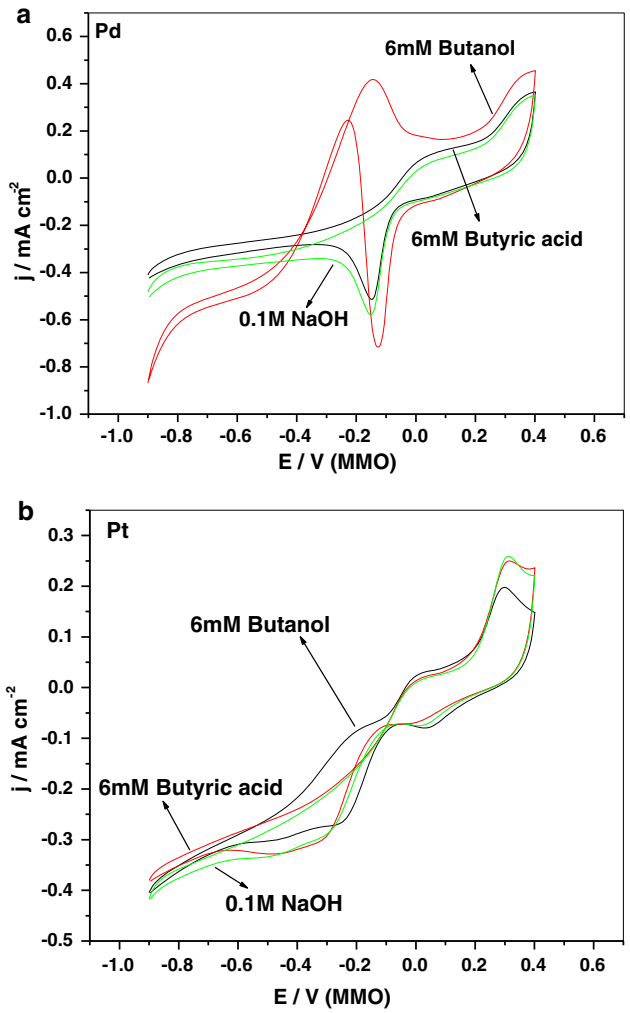

Fig. 7 Cyclicvoltammograms (steady cycle) of butan-1-ol and butanoic acid each at concentration of 6 mM, in 0.1 M NaOH for **a** Pd and **b** Pt electrodes, respectively at scan rate, 50 mV s^{-1}

The Tafel slope on Pt electrode (2.30 V $dec^{-1)}$ is much higher than that on Pd (0.511 V dec^{-1}) electrode at 0.1 M concentration of butan-1-ol in 0.1 M NaOH solution, suggesting more effective electron transmission on catalytically renewable surface of Pd than Pt. However, exchange current density, i_0 values as computed on the basis of Eq. (1) is found to be greater for Pt (0.429 mA cm^{-2}) than that for Pd (0.03 mA cm^{-2}). Since the Tafel slopes/transmission co-efficient and hence mechanisms are different, their electro-catalytic capabilities can not be compared by i_0 values. This is because the current density of Pt is greater than that of Pd at lower potential, but the current density of the later is greater at higher potential, as evident from Fig. 5. The stability of the electrodes in butan-1-ol oxidation has been studied by chronoamperometry (CA) at various concentrations of butan-1-ol using different potentials. Figure 6(a) and (b) for Pd and Pt electrodes represent typical profiles. The chronoamperometric profiles for oxidation of butan-1-ol as shown in the inset of Fig. 6(a), reveals the long time (2 h) stability of Pd and Pt electrodes indicating that the poisoning tolerance of Pd is greater than Pt.

3.3 Study of path of oxidation from CV

In order to get an idea about the path of oxidation of butan-1-ol, CV studies have conducted with both butan-1-ol and n-butyric acids on Pd and Pt electrodes, as depicted in Fig. 7(a) and (b), respectively. The steady CV profiles for 0.1 M sodium hydroxide solution and 6 mM of sodium butyrate in 0.1 M sodium hydroxide almost overlap on one another throughout the potential range indicating that butyrate anion is not oxidized on the electrodes in the medium. The profiles for butan-1-ol oxidation are different from the above-mentioned profiles and show peak for butan-1-ol oxidation on forward scan of potential on both Pd and Pt anodes. As the metal oxide (Pd–O/Pt–O) covers gradually the electrode surface, the oxidation current reduces with increase in potential. When the potential is above +0.15 V for Pd and −0.09 V for Pt the oxidation current including the peak currents nearly coincides with the current of the supporting electrolyte. This indicates that butan-1-ol oxidation is negligible above these respective potentials for Pd and Pt and so the oxidation current at various potentials nearly overlaps with the base current drawn from supporting electrolyte alone in solution. Thus, the study indicates that oxidation of butyrate ion on both the electrodes is negligible. Several other studies also show that cleavage of C–C bond is rather difficult on the Pd and Pt catalyst [29, 38–44]. Therefore the main nonpoisonous product found is thought to be butyrate anion as supported by the subsequent FTIR study.

3.4 FTIR study of the products

It is observed that for Pd electrode, (Fig. 8(a); Table 1), no band appears between wave number 1680–1620 cm^{-1} for C=C stretching, so the possibility of butene formation by dehydration of butan-1-ol does not occur like acid medium [45]. The presence of carbonyl (C=O) group, symmetrical stretching of C–O bond, carbonate, and carboxylate anion [45–48] indicate that both butanoate and carbonate ions formation may occur due to the electrochemical oxidation of butan-1-ol on Pd electrode. In Fig. 8(b), the appearance of two weak absorption peaks on the left of 2700 and 2800 cm^{-1} and peaks around 1740–1720 cm^{-1} (Table 1), indicates the presence of aldehyde group which may arise following path (2) of Scheme 2. A small absorption band at 1647 cm^{-1} suggests the presence of C=C stretching due to

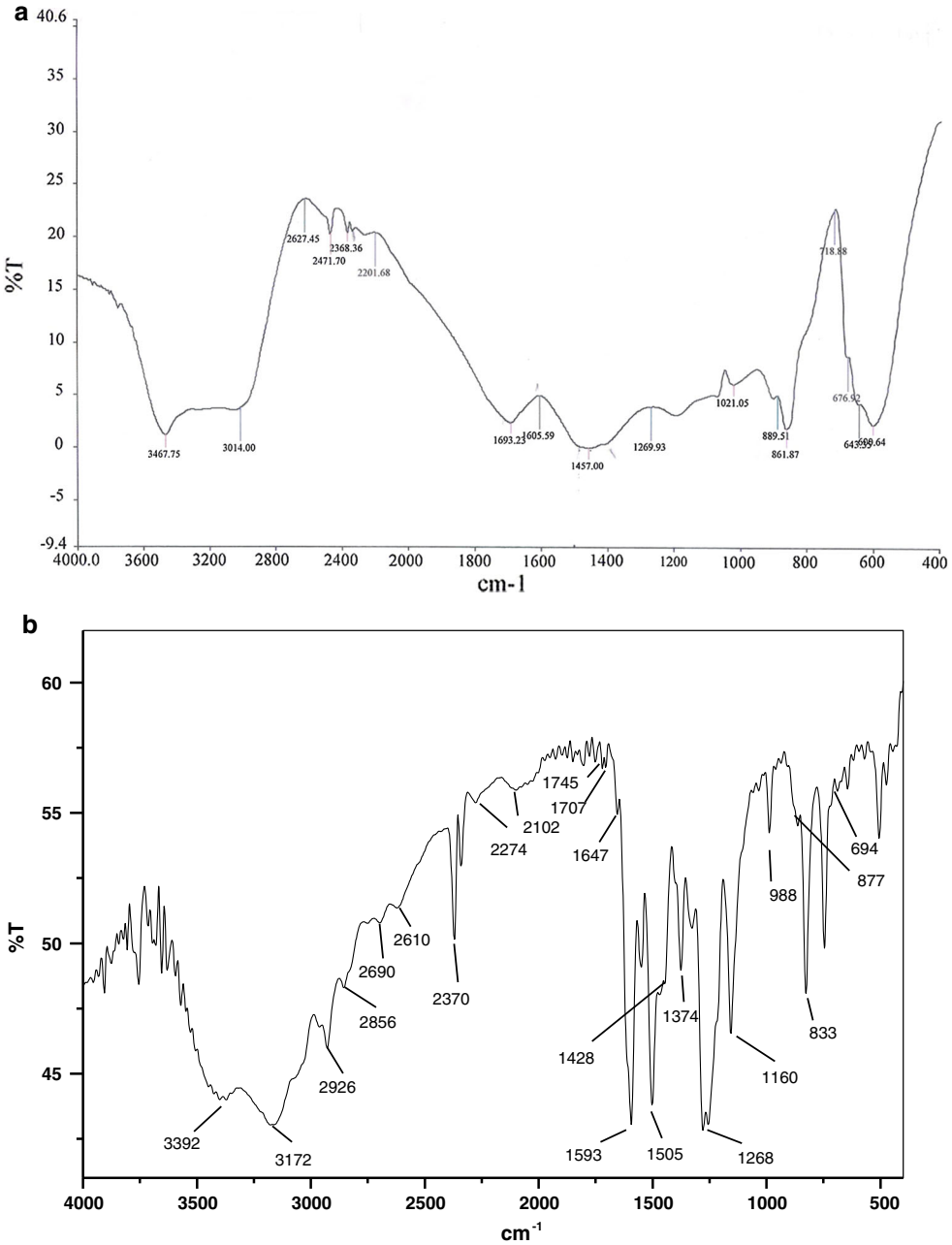

Fig. 8 FT IR spectrum of electro-catalytic oxidation product of 0.1 M butan-1-ol in 0.1 M NaOH for **a** Pd and **b** Pt electrodes, respectively

the formation of butane/alkene which may be generated from intermediate II of Scheme 2 during oxidation of butan-1-ol. Bands between 1760 and 1690 cm^{-1} and weak peaks around 1428, 877, and 694 cm^{-1} indicate the presence of both butanoate and carbonate ions, respectively. So it can be suggested that the Pd electrode follows path (1) and Pt electrode follows path (2) or (3) of Scheme 2.

3.5 Scheme 2

It is generally accepted that primary alcohol is oxidized through both dissociative and non-dissociative adsorption pathways leading to the formation of intermediate (I) and (II) respectively [48, 49]. Intermediate (I) then either form strained surface intermediate (III) leading to the formation of carboxylate anion or form carboxylic acid which subsequently converts to either carboxylate anion or a cyclic ketone (IV) leading to strained cyclic compound (V) and M–CO (poisonous or nonpoisonous) (VI), which appear at high potential. In the dissociative path, primary alcohol first produces cyclic surface intermediate (II) leading to (V) and (VI) which act as precursors of the final product, CO_3^{2-} ion as well as poison to such reaction.

Table 1 Assignments of main FTIR bands observed from spectra of the products of butan-1-ol oxidation

Pd electrode		Pt electrode	
Wave number (cm^{-1})	Possible assignment	Wave number (cm^{-1})	Possible assignment
3002	C–H symmetrical stretching of $–CH_3$	Left of 2700 and 2800 and 1740–1720	–CHO
1693	Carbonyl (C=O)	1760–1690	Butanoate
1457	Deformation of C–H bond	1647	C=C stretching
Intense broad band at 1457 (1485,1457,1396)	Carboxylate		
862	Carbonate	1428, 877, 694	Carbonate
1195	Symmetrical stretching of C–O bond		
1021	$–CH_3$ rocking		

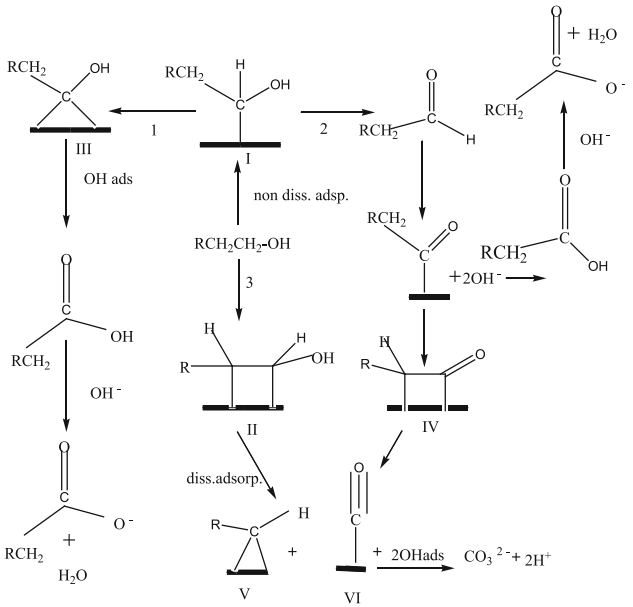

Scheme 2 Generalised mechanistic pathway for oxidation of alcohol on Pt and Pd in alkaline medium

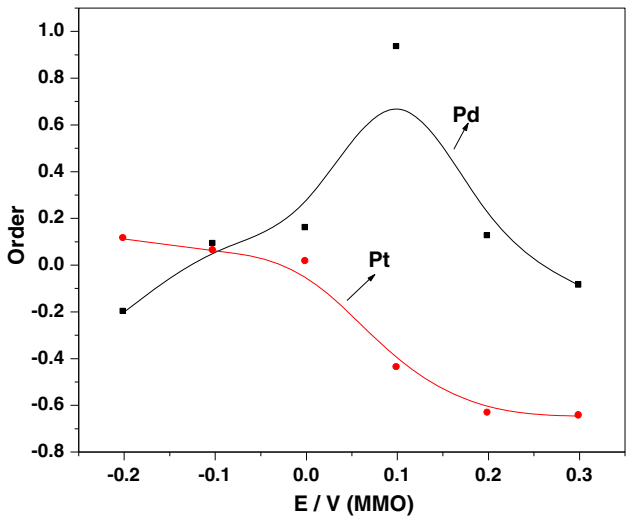

Fig. 9 Plot of Order (with respect to butan-1-ol) versus potential for Pd and Pt electrode

3.6 Order with respect to butan-1-ol

The order with respect to any species (k) is defined as the change in natural logarithm of current density (i) with change in natural logarithm of concentration (C_k) of the species (k) in solution when concentrations of all other species in the solution, electrode solution potential difference ($\Delta\varphi$) and temperature remain same. Thus, the order of butan-1-ol is determined at various potential using the equation: $\rho_{\text{butanol}} = (\partial \log i/\partial \log C_k)_{\Delta\varphi}$, c_{OH^-} and is found to be potential and concentration dependent. The order is found to change with potential in different ways (Fig. 9) for Pt and Pd. On increasing potential from −0.2 to 0.3 V the order gradually decreases for Pt from a positive value to a negative one while for Pd, order sharply increases from a negative value to a maximum at ca. 0.1 V and subsequently decreases to a negative value at ca. 0.3 V. The results may be inferred that for Pt butan-1-ol undergoes partial oxidation with limited adsorption of poisoning intermediate at the lower potential following non-dissociative adsorption pathway, but accumulates large amount of poisoning intermediate by following dissociative adsorption pathway in course of complete oxidation to form CO_3^{2-} and H_2O at higher potential. This inference is consistent with the fact that Pt is known as the best metal catalyst for dehydrogenation of small organic molecules at lower potential, but susceptible to poisonous intermediates at higher potential [50]. In contrary, Pd is relatively less capable of dehydrogenation of butan-1-ol both at lower and higher potential compared to Pt, but with the rise of potential more oxophilic Pd easily forms

intermediate like $Pd(OH)_n$ ($n = 1, 2$) [48] which at low potential reacts with non-dissociative adsorbed butan-1-ol to form butyric acid instead of complete oxidation product by different pathways as shown in Scheme (2). At high potential, however, it also undergoes dissociative adsorption paths leading to the formation of strained molecules and M–CO resulting poisoning.

4 Conclusion

Pure Pd is found to be a better electro-catalyst than the conventional catalyst, pure Pt above −0.18 V versus MMO, for steady-state oxidation of butan-1-ol in 0.1 M aqueous NaOH solution. Tafel slope on Pt electrode is greater and Pt is poisoned at lower potential compared to Pd. Formation of several intermediates containing alkene and aldehyde groups is evident from FTIR study with Pt electrode unlike Pd, indicating different mechanistic paths of oxidation of butan-1-ol resulting relatively lower activity of Pt than Pd electrode. The order with respect to butan-1-ol gradually decreases with increase of potential for Pt due to poisoning in the process of formation of complete oxidation product, CO_3^{2-} ,but increases up to a limit for Pd which follows a different paths with the major formation of butyrate. The experimental results conform to the proposed mechanisms given by Scheme 2.

References

1. Barragan VM, Heinzel A (2002) Estimation of the membrane methanol diffusion coefficient from open circuit voltage measurements in a direct methanol fuel cell. J Power Sources 104:66–72
2. Tang HL, Wang SL, Pan M, Jiang SP, Ruan YZ (2007) Performance of direct methanol fuel cells prepared by hot-pressed MEA and catalyst-coated membrane (CCM). J Electrochim Acta 52:3714–3718
3. Heinzel A, Barragan VM (1999) A review of the state of the art of the methanol crossover in direct methanol fuel cell. J Power Sources 84:70–74
4. Ren X, Springen TE, Zawodzmski TA, Gottegfeld S (2000) Methanol transport through Nafion membranes. Electro-osmotic drag effects on potential step measurements. J Electrochem Soc 147(2):466–474
5. Dillion R, Srinivasan S, Arico AS, Antonucci V (2004) International activities in DMFC R&D: status of technologies and potential applications. J Power Sources 127:112–126
6. Paul P, Bagchi J, Bhattayacharya SK (2006) Electrochemical oxidation of ethanol on thin coating on platinum based material on nickel support. Indian J Chem 45:1144–1152
7. Mauritz KA, Moore RB (2004) State of understanding of nafion. Chem Rev 104:4535–4586
8. Ye J, Liu J, Xu C, Jiang SP, Tong Y (2007) Electrooxidation of 2-propanol on Pt, Pd and Au in alkaline medium. Electrochem Commun 9:2760–2763
9. Liu J, Ye J, Xu C, Jiang SP, Tong Y (2008) Electro-oxidation of methanol, 1-propanol and 2-propanol on Pt and Pd in alkaline medium. J Power Sources 177:67–70
10. Takky D, Beden B, Leger JM, Lamy C (1988) Evidence for the effect of molecular structure on the electrochemical reactivity of alcohols: part III. Electro-oxidation of the butanol isomers on platinum single crystals in an alkaline medium. J Electroanal Chem 256:127–136
11. Xu CW, Shen PK (2005) Electrochamical oxidation of ethanol on Pt–CeO_2/C catalysts. J Power Sources 142:27–29
12. Tripkovic AV, Popovic KD, Lovic JD, Jovanovic VM, Kowal A (2004) Methanol oxidation at platinum electrodes in alkaline solution: comparison between supported catalysts and model systems. J Electroanal Chem 572:119–128
13. Rodrigues IA, Nart FC (2006) 2-Propanol oxidation on platinum and platinum–rhodium electrodeposits. J Electroanal Chem 590:145–151
14. Otomo J, Li XE, Kobayashi T, Wen CJ, Nagamoto H, Takahashi H (2004) AC-impedance spectroscopy of anodic reactions with adsorbed intermediates: electro-oxidations of 2-propanol and methanol on carbon-supported Pt catalyst. J Electroanal Chem 573:99–109
15. Guo JW, Zhao TS, Probhuram J, Chen R, Wong CW (2006) Development of PtRu–CeO_2/C anode electrocatalyst for direct methanol fuel cells. J Power Source 156:345–354
16. Zhang LL, Lu TH, Bao JC, Tag YW, Li C (2006) Preparation method of an ultra fine carbon supported Pd catalyst as an anodic catalyst in a direct formic acid fuel cell. Electrochem Commun 8:1625–1627
17. Ji XB, Banks CE, Xi W, Wilkinas SJ, Compton RG (2006) Edge plane sites on highly ordered pyrolytic graphite as templates for making palladium nanowires via electrochemical decoration. J Phys Chem B 110:22306–22309
18. Savadogo O, Lee K, Oishi K, Mitsushima S, Kamiya N, Ota KI (2004) New palladium alloys catalyst for the oxygen reduction reaction in an acid medium. Electrochem Commun 6:105–109
19. Bagchi J, Bhattayacharya SK (2008) Studies of the electrocatalytic activity of binary palladium ruthenium anode catalyst on Ni support for ethanol alkaline fuel cells. Trans Met Chem 33:113–120
20. Beden B, Leger JM, Lamy C, Bockris JOM, Conway BE, White RE (eds) (1992) Modern aspect of electrochemistry (chapter 2), vol 22. Plenum Press, New York
21. Prabhuram J, Manoharan R (1998) Investigation of methanol oxidation on unsupported platinum electrodes in strong alkali and strong acid. J Power Sources 74:54–61
22. Tripkovic AV, Popovic KD, Momcilovic JD, Drazic DM (1996) Kinetic and mechanistic study of methanol oxidation on a Pt(111) surface in alkaline media. J Electroanal Chem 418:9–20
23. Tripkovic AV, Popovic KD, Momcilovic JD, Drazic DM (1998) Kinetic and mechanistic study of methanol oxidation on a Pt(100) surface in alkaline media. J Electroanal Chem 448:173–181
24. Tripkovic AV, Popovic KD, Momcilovic JD, Drazic DM (1998) Kinetic and mechanistic study of methanol oxidation on a Pt(110) surface in alkaline media. Electrochim Acta 44:1135–1145
25. Tripkovic AV, Popovic KDj, Lovic JD (2001) The influence of the oxygen-containing species on the electrooxidation of the C1–C4 alcohols at some platinum single crystal surfaces in alkaline solution. Electrochim Acta 46:3163–3173
26. Yu EH, Scott K, Reeve RW (2003) A study of the anodic oxidation of methanol on Pt in alkaline solutions. J Electroanal Chem 547:17–24

27. Garden M, Kotowski J, Czerwinski A (2000) The study of electrochemical palladium behavior using the quartz crystal microbalance. J Solid State Electrochem 4:273–278
28. Garden M, Czerwinski A (2008) EQCM studies on Pd–Ni alloy oxidation in basic solution. J Solid State Electrochem 12:375–385
29. Liang ZX, Zhao TS, Xu JB, Zhu LD (2009) Mechanism study of the ethanol oxidation reaction on palladium in alkaline media. Electrochim Acta 54:2203–2208
30. Hildenbrad DL, Lau KH (2000) Dissociation energy of the PdO molecule. Chem Phys Lett 319:95–98
31. Yatsuhisa N (2002) Standard enthalpy of formation of platinum hydrous oxide. J Therm Anal Calorim 69:831–839
32. Trasatti S, Petrii OA (1991) Real surface area measurements in electrochemistry. Pure Appl Chem 63(5):711–734
33. Singh RN, Singh A (2009) Electrocatalytic activity of binary and ternary composite films of Pd, MWCNT and Ni, part II: methanol electrooxidation in 1 M KOH. Int J Hydrogen Energy 34(4):2052–2057
34. Mahapatra SS, Dutta J (2011) Characterization of Pt–Pd/C electrocatalyst for methanol oxidation in alkaline medium. Int J Electrochem. doi:10.4061/2011/563495
35. Morin MC, Lamy C, Leger JM (1990) Structural effects in electrocatalysis: oxidation of ethanol on platinum single crystal electrodes. Effect of pH. J Elerctronal Chem 283:287–302
36. Huang JC, Liu ZL, He CB, Gan LM (2005) Synthesis of PtRu nanoparticles from the hydrosilylation reaction and application as catalyst for direct methanol fuel cell. J Phys Chem B 109:16644–16649
37. Bard AJ, Faulkner LR (1980) Electrochemical methods: fundamentals and applications (chapter 11: electrode reactions with coupled homogeneous chemical reactions). Wiley, New York
38. Shen PK, Xu CW (2006) Alcohol oxidation on nanocrystalline oxide Pd/C promoted electrocatalysts. Electrochem Commun 8:184–188
39. Liu HP, Ye JP, Xu CW, Jiang SP, Tong YX (2007) Kinetics of ethanol electrooxidation at Pd electrodeposited on Ti. Electrochem Commun 9:2334–2339
40. Nie M, Tang HL, Wei ZD, Ziang SP, Shen PK (2007) Highly efficient AuPd–WC/C electrocatalyst for ethanol oxidation. Electrochem Commun 9:2375–2379
41. Xu CW, Cheng LQ, Shen PK, Liu YL (2007) Methanol and ethanol electrooxidation on Pt and Pd supported on carbon microspheres in alkaline media. Electrochem Commun 9:997–1001
42. Zheng HT, Li YL, Chen SX, Shen PK (2006) Effect of support on the activity of Pd electrocatalyst for ethanol oxidation. J Power Source 163:371–375
43. Bagchi J, Bhattacharya SK (2007) Electrocatalytic activity of binary palladium ruthenium anode catalyst on Ni-support for ethanol alkaline fuel cells. Transit Met Chem 32:47–55
44. Zhou ZY, Wang Q, Lin JL, Tian N, Sun SG (2010) In situ FTIR spectroscopic studies of electrooxidation of ethanol on Pd electrode in alkaline media. Electrochim Acta 55:7995–7999
45. Li NH, Gang SS (1997) In situ FTIR spectroscopic studies of the electrooxidation of C_4 alcohol on a platinum electrode in acid solutions part I. Reaction mechanism of 1-butanol oxidation. J Electroanal Chem 436:65–72
46. Nakomoto K (1986) Infrared and Raman spectra of inorganic and co-ordination compounds. Wiley, New York
47. Andrzej K, Simon NP, Richard JN (1997) Nickel hydroxide electrocatalysts for alcohol oxidation reactions: an evaluation by infrared spectroscopy and electrochemical methods. Catal Today 38:483–492
48. Lin-Vien D, Colthup NB, Fately WG, Grasselli JG (1991) The hand book of infrared and Raman characteristic frequencies of organic molecules. Academic Press, New York
49. Bianchini C, Shen PK (2009) Palladium-based electrocatalysts for alcohol oxidation in half cells and in direct alcohol fuel cells. Chem Rev 109:4183–4206
50. Bagchi J, Bhattacharya SK (2007) The effect of composition of Ni-supported Pt–Ru binary anode catalysts on ethanol oxidation for fuel cells. J Power Sources 163:661–670